Int. J. Electrochem. Sci., 8 **(2013)** 12566 - 12579

International Journal of
ELECTROCHEMICAL
SCIENCE
www.electrochemsci.org

Influence of Anion and pH on the Electrochemical Co-Deposition and Transformation of Iron Oxy-Hydroxide

P. Montoya, T. Marín, A. Echavarría, J. A. Calderón[*]

Centro de Investigación, Innovación y Desarrollo de Materiales –CIDEMAT, Universidad de Antioquia. Medellín, Colombia
[*]E-mail: jacalder@udea.edu.co

Received: 16 August 2013 / *Accepted:* 4 October 2013 / *Published:* 20 October 2013

Goethite (α-FeOOH) and lepidocrocite (γ-FeOOH) are two common iron and steel corrosion products. The study of goethite and lepidocrocite is an interesting way to better understand the corrosion processes of iron and its behaviour in different environments. In this work the co-deposition of iron oxides and their transformation on inert subtracts were studied at room temperature. The films were obtained by electro-deposition using solutions containing Cl^-, SO_4^{2-} and Fe^{2+}at different pH on platinum disks. Linear polarisation, amperommetry, electrochemical impedance and spectroscopy techniques were used in this study. Anodic polarisation curves showed a current shoulder at low anodic polarisation and a current peak at higher polarisation. The shoulder observed at low anodic polarisation corresponded to the formation of a precursor compound like Fe^{2+}-Fe^{3+} hydrated oxide, which is later transformed to an oxy-hydroxide compounds. The electrodeposition of goethite and lepidocrocite occurs, firstly through formation of a green rust film, characterised by a shoulder in the polarisation curves, and subsequently through formation of an iron oxy-hydroxide film. The anion and the pH of the electrolyte played an important role in the formation and further transformation of the iron oxides compounds on the film. It was corroborated that the Cl^- ions and high pH stimulated the green rust and final oxyhydroxide film formation, while the SO_4^{2-} ions and low pH retarded the formation of these compounds.

Keywords: iron oxides electrodeposition, goethite, lepidocrocite, corrosion products.

1. INTRODUCTION

Goethite (α-FeOOH) and lepidocrocite (γ-FeOOH) are two common products of iron and steel corrosion. However, their properties and role in the corrosion of metals are very different. The composition of rust formed on steel exposed to the atmosphere is even more complex, as it depends on environmental conditions such as weathering processes and the presence of atmospheric polluting

agents; therefore it is possible to form numerous corrosion products with different characteristics [1]. In addition, other oxy-hydroxides like akaganeite (β-FeOOH) and iron oxides such as magnetite (Fe_3O_4) and maghemite (γ-Fe_2O_3) can be formed during iron corrosion in the atmosphere. The study of goethite and lepidocrocite can help to reveal the corrosion processes and behaviour of iron and steel in different environments.

Knowledge of the role of each rust constituent in the phenomenon of steel corrosion is not easy to acquire due to the complexity of rusting. Many rust constituents have been obtained by hydrothermal synthesis, enabling the study of their properties and the effect of the addition of some elements to their structure [2,3]. Hydrothermal synthesis is the technique most commonly used to obtain iron compounds. However, in recent years other techniques have been used to obtain thin films of iron oxides, in order to facilitate their individual study. These include pulsed laser deposition or laser ablation deposition [4], chemical vapour deposition [5], wet chemical deposition [6], sol-gel deposition [7,8] and sputtering [9]. Electrochemical synthesis is an alternative method that presents economic advantages in sample preparation due to minimum consumption of reagents. The electrodeposition technique has huge advantages over the hydrothermal process, mainly in the preparation of films. In electrochemical synthesis, the thickness, morphology and composition of the films can be controlled by the applied voltage and the current density. Using this method it is possible to obtain thin layers of iron corrosion products on a conductive surface [10-13]. The electrochemical synthesis of green rusts GR1 and GR2 using solutions containing Cl^-, SO_4^{2-} and CO_3^{2}- was reported by Peulon [10]. Pure and mixed products of good crystalinity were obtained. Other iron oxides and oxy-hydroxides obtained electrochemically on inert surfaces, were also reported [11,12]. These syntheses were carried out by changing the local pH and the metal oxidation states of the ion Fe^{2+}. Peulon synthesised Lepidocrocite from green rust and, also, by direct oxidation. However, the co-deposition of goethite occurred when the synthesis temperature was grater than 20°C [12]. Recently Chung *et al* reported the synthesis of nano structural films of iron oxides [13]. In that work, films of duplex oxides/oxy-hydroxides of iron were obtained by electrochemical synthesis of green rust from ammonia solutions and further chemical oxidation. Génin *et al* studied the thermodynamic stability of green rusts GR1 and GR2 and reported the potential–pH diagrams for the rusts [$3Fe(OH)_2.Fe(OH)_2Cl.nH_2O$] [14], [$Fe_4^{(II)}Fe_2^{(III)}(OH)_{12}$].[$CO_3.2H_2O$] [15] and [$Fe_4^{(II)}Fe_2^{(III)}(OH)_{12}]^{2+}$.[$SO_4.2H_2O]^{2-}$ [16]. The authors reported the formation of green rust and that its subsequent oxidation to goethite or lepidocrocite depended on the relationships [anion]/[OH^-] and [Fe^{2+}]/[OH^-].

In atmospheric corrosion of iron, the initial oxidation of green rust and subsequent oxidation to more stable compounds such as lepidocrocite and goethite is a common process. In this process, the pH of the water layer and the type of anions coming from pollutants, such as Cl^- and SO_4^{2-}, have an important role, inducing or inhibiting the transformations of certain oxyhydroxides. This work seeks to contribute to the better understanding of the formation processes of some commonly found compounds during the corrosion of iron in the atmosphere and the influence of variables like pH, Cl^- and SO_4^{2-} anions on their transformation into other compounds.

2. EXPERIMENTAL

Sodium chloride (NaCl, analytic grade chemical, Merck), sodium sulphate (Na_2SO_4, analytic grade chemical, Merck), 1-methyl-imidazole (99%, Aldrich), iron chloride ($FeCl_2.4H_2O$, GR, Merck) and HCl (36.5-38%, J.T. Baker) were used for electrochemical synthesis. The solutions were prepared with ultra pure water (conductivity 0.0054 $\mu S.cm^{-1}$) and then deaerated with nitrogen. The electrochemical synthesis was done in a 120 mL glass cell equipped with an Ag/AgCl (0.1M NaCl) reference electrode and a platinum cylindrical grill of 20 cm^2 of area as counter electrode. A platinum disk of 15 mm diameter was used as working electrode. Before each experiment the working electrode was mechanically polished until a standard grade of 1200 was reached and subsequently polished with a cloth with the addition of alumina until a reflective surface was obtained. The pH of the solution was measured with a METROHM combined pH electrode. Temperature was maintained between 24 and 25 ºC. The potential values given in this work are always versus Ag/AgCl.

2.1. Preparation of the electrolytes

The electrolytic solutions were prepared following the general procedure already described [10]. Chloride media (0.1M 1-methyl-imidazole + 0.4M NaCl) and sulphate media (0.1M 1-methyl-imidazole + 0.2M Na_2SO_4) were prepared at room temperature. The initial pH of the solution was close to 10. Thereafter, 30 mL of electrolyte was added into the cell and the solution was deaerated in nitrogen atmosphere for approximately 30 minutes. Then, 1 mL of 0.41M $FeCl_2.4H_2O$, as Fe^{2+} source, was added to the solution and the system was allowed to stabilise for 15 minutes. Finally, the pH was carefully adjusted to 7 or 8 by adding of 1M HCl. The system was kept in nitrogen throughout the electrochemical synthesis.

2.2. Electrochemical tests

The kinetic of iron oxy-hydroxide film formation on platinum electrode was studied by potentiodynamic polarisation. Polarisation curves were recorded for each chloride and sulphate electrolytes at different pH values, starting at the open circuit potential (OCP) until 1 V of anodic overpotential. The sweeping speed of potentiodynamic test was $1.666 \times 10^{-4} V\ s^{-1}$. Additionally, films of iron oxy-hydroxides were obtained by potentiostatic polarisation at potentials especially selected from the potentiodynamic curves, using solutions of SO_4^{2-} and Cl^- at pH 7 and 8. The electrochemical depositions were carried out for approximately 180 minutes. During the electrochemical deposition, current transients (I *vs* t) were recorded in order to monitor the stability and growth of the deposits. The films obtained after each experiment were washed with ultra pure water and dried with nitrogen. Electrochemical impedance (EIS) spectra were obtained during the electrodeposition. Potentiostatic control was used for EIS measurements at potentials selected from the polarisation curves. EIS measurements were carried out at 10 mV amplitude using a range of frequencies between 60 kHz to 50

mHz. All the electrochemical tests were made using a potentiostat-galvanostat BAS–ZAHNER IM6e with impedance analyzer controlled by THALES software.

2.3. Films characterisation

Fourier Transform Infrared Spectroscopy (FTIR) was carried out using a Thermo Smart diffuse reflectometer (Nicolet avator 330 FT–IR). The surface morphology and particle sizes were observed by Scanning Electron Microscopy (SEM) JEOL JSM-5910LV and by optic microscope (NIKON ECLIPSE E200 POL). Micro-Raman spectroscopy was done using a Horiba Jobin Yvon model Labram HR spectrometer. The micro-Raman spectrometer was doted with a diode laser of 785 nm, with spot size of 1 to 300 μm. The time o exposition was set between 25 to 50 seconds.

3. RESULTS AND DISCUSSION

3.1. Polarisation curves

Figure 1 shows the anodic polarisation curves obtained during the electrodeposition of iron oxy-hydroxides films. All the curves present similar behaviour; very low anodic potentials produce a slight increase of current, followed by a sharp increase once intermediate potentials are reached, at which point the shoulder is formed. Then, at higher anodic potentials the current increases again, producing a peak, after which a progressive decline of current is presented. The behaviour observed in the polarisation curves can be explained by the formation of iron oxide compounds on the electrode surface. This was similar in all conditions, except for electrodeposition in sulphate electrolyte at pH 7 (Figure 1a), where there was no clear evidence of shoulder formation.

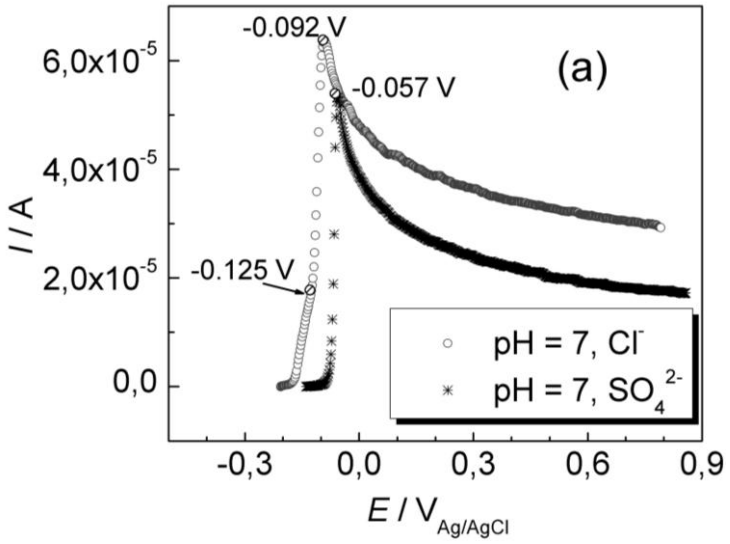

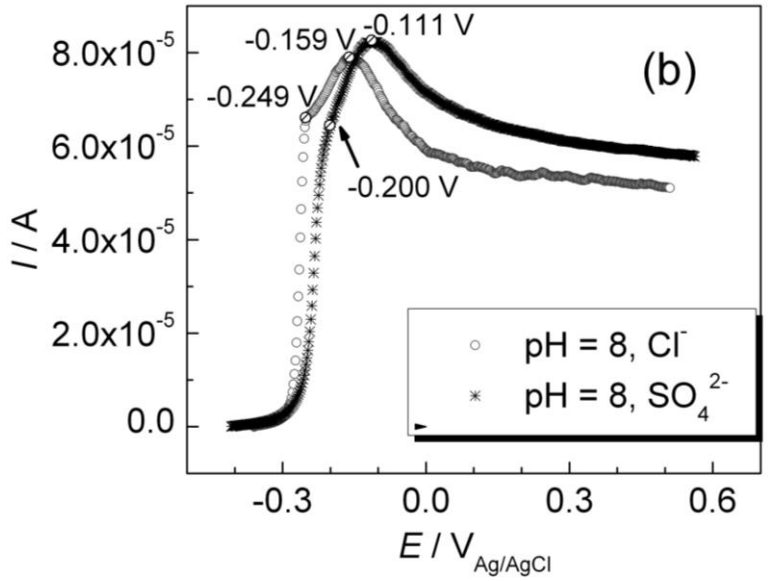

Figure 1. Anodic polarisation curves during the iron oxyhydroxides electrodeposition in chloride (0.1M 1-methyl-imidazole + 0.4 NaCl) and sulphate (0.1M 1-methyl-imidazole + 0.2M Na_2SO_4) media, (a) pH = 7 and (b) pH = 8.

In chloride media the formation of a green film was observed during polarisation at potential values close to the shoulder potential. The transformation of this film into an orange product was observed at potential values close to the potential of the current peak. Similarly, in sulphate media, the transformation of the deposit from a yellow film to a dark orange film was observed at potentials values close to the potential of the current peak.

The characteristic potentials of the current shoulder and peak presented in the polarisation curves for different conditions are shown in Table 1. It can be seen that the current shoulder and peak at pH 8 are formed at lower anodic potentials than those formed at pH 7. Similarly, lower values of anodic polarisation are required for the formation of the shoulder and current peak in chloride media, compared to those required for sulphate.

Table 1. Characteristic potentials of the shoulder and current peak showed in the polarization curves during the iron oxyhydroxides electrodeposition in chloride (0.1M 1-methyl-imidazole + 0.4 NaCl) and sulphate (0.1M 1-methyl-imidazole + 0.2M Na_2SO_4) electrolyte.

Anion	pH			
	7.0		8.0	
	Shoulder	Peak	Shoulder	Peak
Cl^-	-0.125V	-0.092V	-0.249V	-0.159V
SO_4^{2-}	---	-0.057V	-0.200V	-0.111V

This indicates that the compounds responsible for the formation of the shoulder and the current peak during the electrodeposition process are stimulated by high pH and Cl^- ions rather than low pH

values and SO_4^{2-} ions. The potential values of the shoulder observed in the polarisation curves are at the limit of the region within which green rusts are stable. This agrees with the potential/pH diagrams reported in the literature [14-16]. Likewise, the potential values of the current peak observed in the polarisation curves are in the regions in which lepidocrocite [14,16] and goethite [15] are formed and are stable.

Figure 2 shows the ammperometry curves corresponding to the transients I *vs* t, recorded during potentiostatic polarisation at the current peak potentials for the different systems evaluated. Initially, the current rises to values greater than those of the current peak observed in the polarisation curves, except for chlorides at pH 7, where the initial current remains similar to the current peak. Afterwards, the current decreases quickly until it reaches an almost stable plateau. Regarding this point, it is suggested that the low conductivity of the oxide film and the barrier effect caused by the film reduce the subsequent oxidation of Fe^{2+}ions diminishing the active sites and determine the value of the current at the plateau. When the oxide film is formed, the process is no longer controlled by the kinetics of the charge transfer process, but by the diffusion of the electroactive species through the film. This phenomenon is corroborated by electrochemical impedance, and it will discuss below.

In the transients I *vs* t curves made in both Cl^- and SO_4^{2-} media, smaller current values were observed at pH 7 than at pH 8, indicating that it is more difficult to form a film at lower pH. Also, little influence of the anion was observed at pH 7 in the transients I *vs* t, as can be seen by the current plateau formation, which was reached in approximately 25 minutes. In contrast, at pH 8 the presence of the Cl^- ion resulted in the current plateau appearing more rapidly (5 minutes) than in SO_4^{2-} media. In SO_4^{2-} media the plateau was reached after 100 minutes of polarisation. Thus means the steady state of the system is more quickly reached in chloride media.

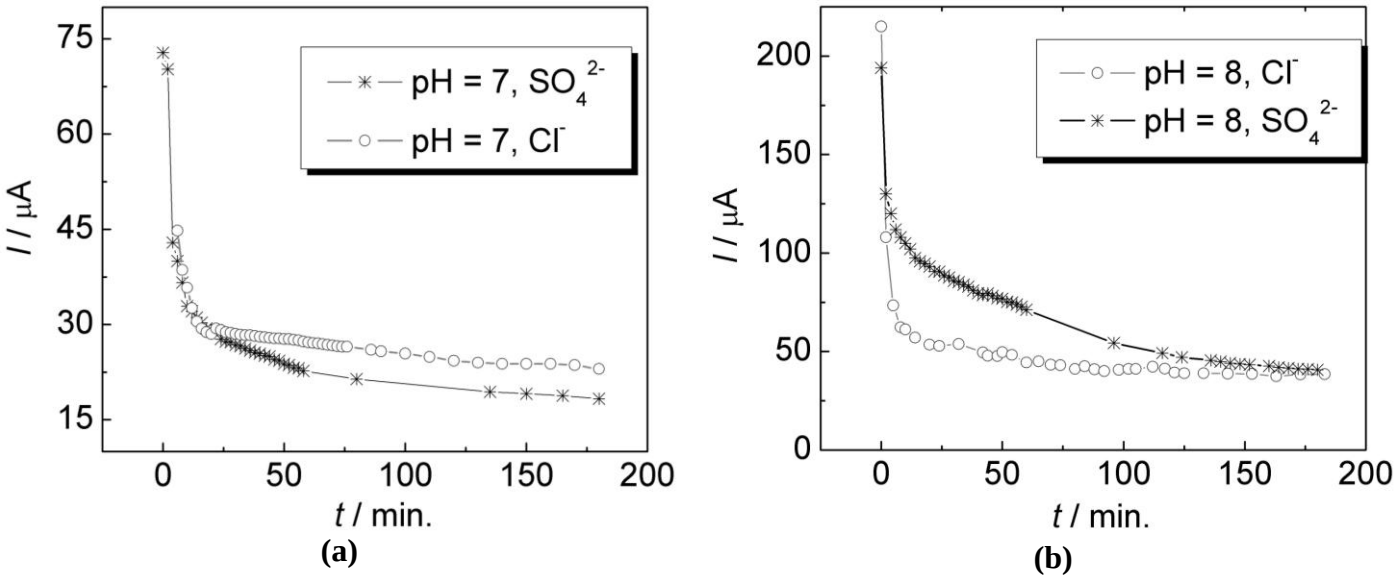

Figure 2. Amperommetric curves corresponding to the transient I – t obtained during the potentiostatic polarisation in the potential of current peak in chloride (0.1M 1-methyl-imidazole + 0.4 NaCl) and sulphate (0.1M 1-methyl-imidazole + 0.2M Na_2SO_4) media, (a) pH = 7 and (b) pH = 8.

These results are consistent with those already saw in polarisation curves. Therefore, the synthesis conditions, defined by the pH and the anion type in the electrolyte, have an important influence on the nucleation and growth of the oxide film, as well as the morphology and homogeneity of the deposits.

3.2. Surfaces Characterisation

3.2.1. FTIR

Figure 3 shows the FTIR spectra of the films electrodeposited using potentiostatic polarisation. For the electrodepositions, the respective over-potential at the current peak was applied for 180 minutes in electrolytes containing ions Cl^- (Figure 3a) and SO_4^{2-} (Figure 3b). The bands at 3370-3384 cm^{-1}, 1600-1640 cm^{-1}, 1400-1410 cm^{-1}, are present at all iron oxide film obtained at different conditions of anion and pH of electrolyte. The high bands at 3370-3384 cm^{-1} is assigned to the O-H stretching vibration (ν_2) commonly found in iron oxyhydroxides compounds [19,20]. The bands at 1600-1640 cm^{-1} arise from hydroxyl bending vibration in water [19,20]. The bands at 1400-1410 cm^{-1} can be assigned to possible contamination of the CO_2 from air or by rest of the 1-methyl-imidazole. Two of the most characteristic bands of goethite or akaganéite (*) at ~898 cm^{-1} and ~696 can be seen at both pH values and Cl^- and SO_4^{2-} electrolytes. The band at ~898 cm^{-1} and 696 can be assigned to OH bending vibration in the mirror plane (100) of goethita [2,19] or akaganéite [21]. On the other hand, in sulphate media, Figure 3(b), the most important bands of lepidocrocite at 1105 cm^{-1}, 1012 cm^{-1} and 735 cm^{-1} can be seen, these bands are not observed in chloride media.

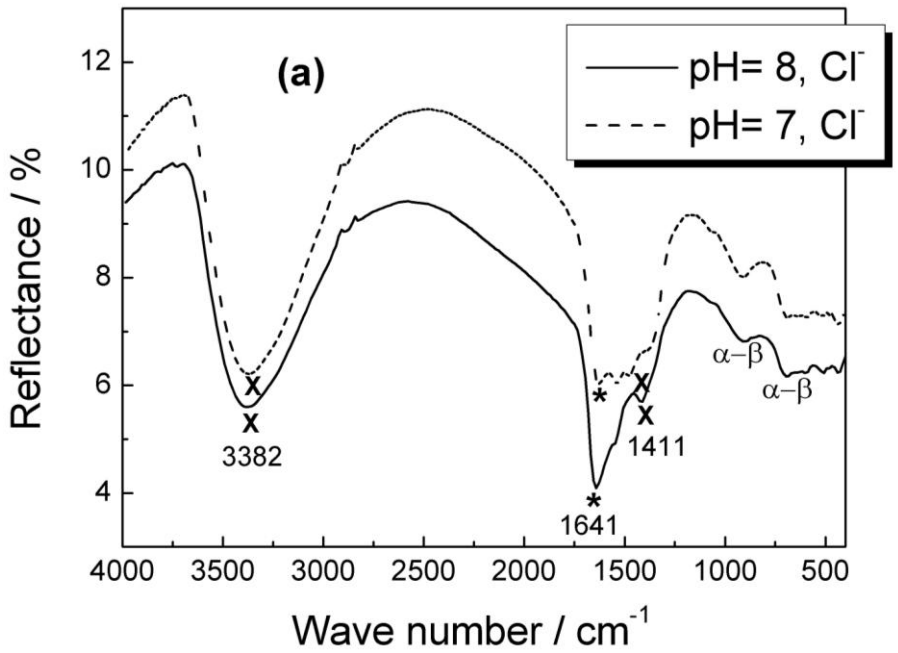

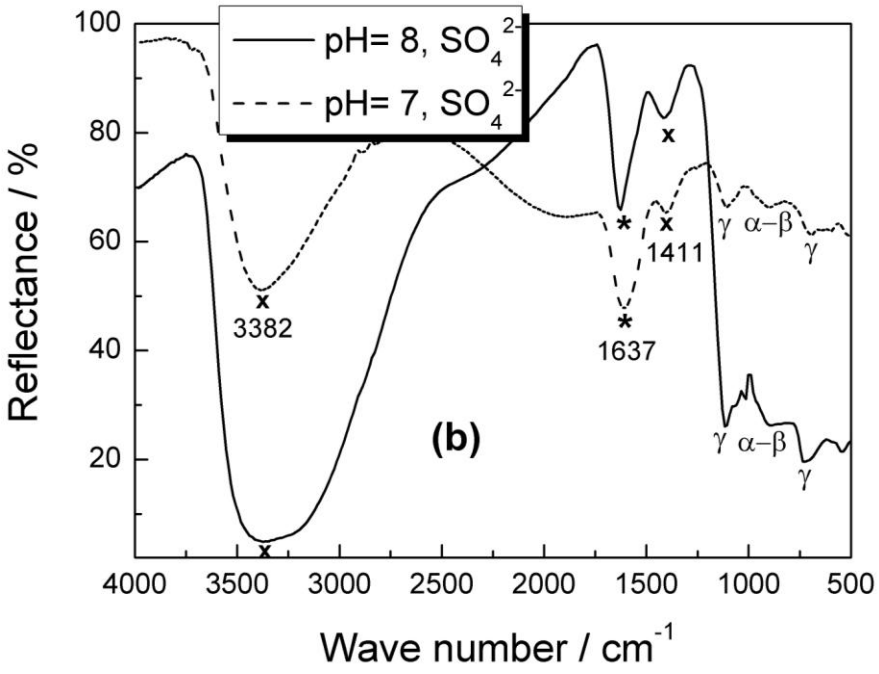

Figure 3. FTIR spectra of the electrodeposited films obtained in (a) chloride (0.1M 1-methyl-imidazole + 0.4 NaCl) and (b) sulphate (0.1M 1-methyl-imidazole + 0.2M Na_2SO_4).

The bands at 1105 cm^{-1} and 1012 cm^{-1} are assigned to OH bending vibration in the plane and the band at 735 cm^{-1} are due to OH bending vibration out of the plane [2, 21]. According to FTIR in chloride media the elctrodeposite film is constitute by goethite and akaganeite, though in sulphate media both lepidocrocite and akaganeite coexist in the film. This is consistent with the work of Génin *et al*, which showed that during the chemical syntheses of GR1, using high levels of Cl^-, the green rust was principally oxidized into goethite, while lepidocrocite was the principal product of oxidation when low levels Cl^- were used. In contrast, in the presence of SO_4^{2-} the oxidation of GR2 always led to lepidocrocite formation [14].

3.2.2. Raman spectroscopy

Figure 4 shows Raman spectra of the films obtained in chloride and sulphate media at pH 8. In order to establish the Raman reference spectrum of each of the possible oxides, pure oxides powders (goethite and lepidocrocite) were synthesized following the hydrothermal methodology described in [2]). Purity of these compounds was also confirmed by X-ray diffraction, no show in this paper. As can be seen in Figure 4, pure goethite and lepidocrocite have a characteristic intense and narrow bands at 250 and 390 cm^{-1} respectively [22- 24]. Others less intense bands appear at 350, 380 and 530 cm^{-1} for lepidocrocite and 239, 300 and 476 cm^{-1} for goethite. A mixture of lepidococite, goethite and akaganeite are present in the electrodeposited films. The presence of akaganeite was confirmed by its characteristic band at 722 cm^{-1} [24, 25]. Although a mixture of these iron oxi-hydroxide are indisputable present in the films obtained in chloride and sulphate media, the bands characteristic of

lepidocrocite are more clearly detected in the films obtained in sulphate, confirming those already saw in FTIR analysis.

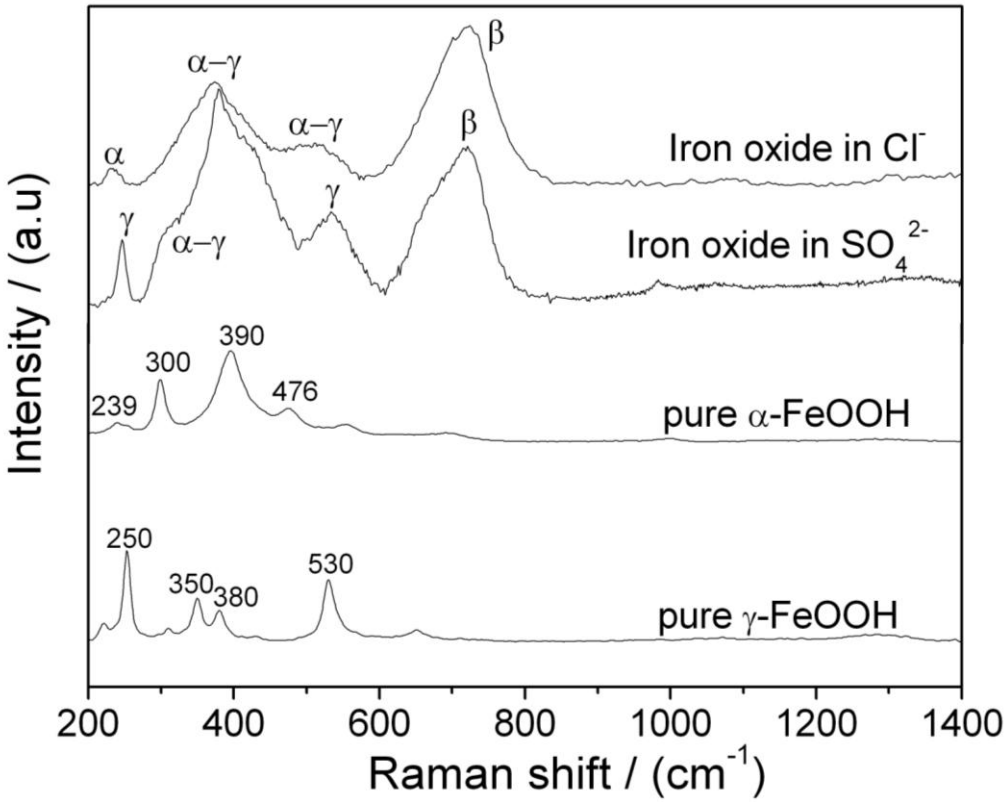

Figure 4. Raman spectra of the electrodeposited films obtained in chloride and sulphate media. It also showed Raman spectra of pure iron oxi-hydroxides.

3.2.3. SEM

Figures 5 and Figure 6 show SEM images of the deposits obtained in sulphate and chloride media, respectively. The images of the deposits for both electrolytes reveal the existence of small acicular shaped crystals at the bottom and the growth of large platelets perpendicular to the substrate with a random orientation on the electrode surface. The principal difference between the deposits obtained at both anions in their respective electrolyte lies mainly in the size of the particles at the bottom of the deposited layer. The deposits obtained at chloride electrolyte have an average particle size of 0.2 μm (Figures 6), while the deposits made at sulphate electrolyte have an average particle size of 1.0 μm (Figures 5). Also, some differences of particle morphology between deposits obtained in the chloride media and those obtained in the sulphate media were observed. In the Cl^- electrolyte the formation of small particles of acicular form was observed at the bottom; however, the particles are arranged in a globular conglomeration (Figures 6 (b) and (d)). In the case for sulphate electrolytes, the particles are arranged manly as plates form. Likewise the pH yields light differences in the particle size

of the deposits. It can be seen in both Cl^- and SO_4^{2-} electrolyte the particles at the bottom are again smaller at pH 7 than at pH 8.

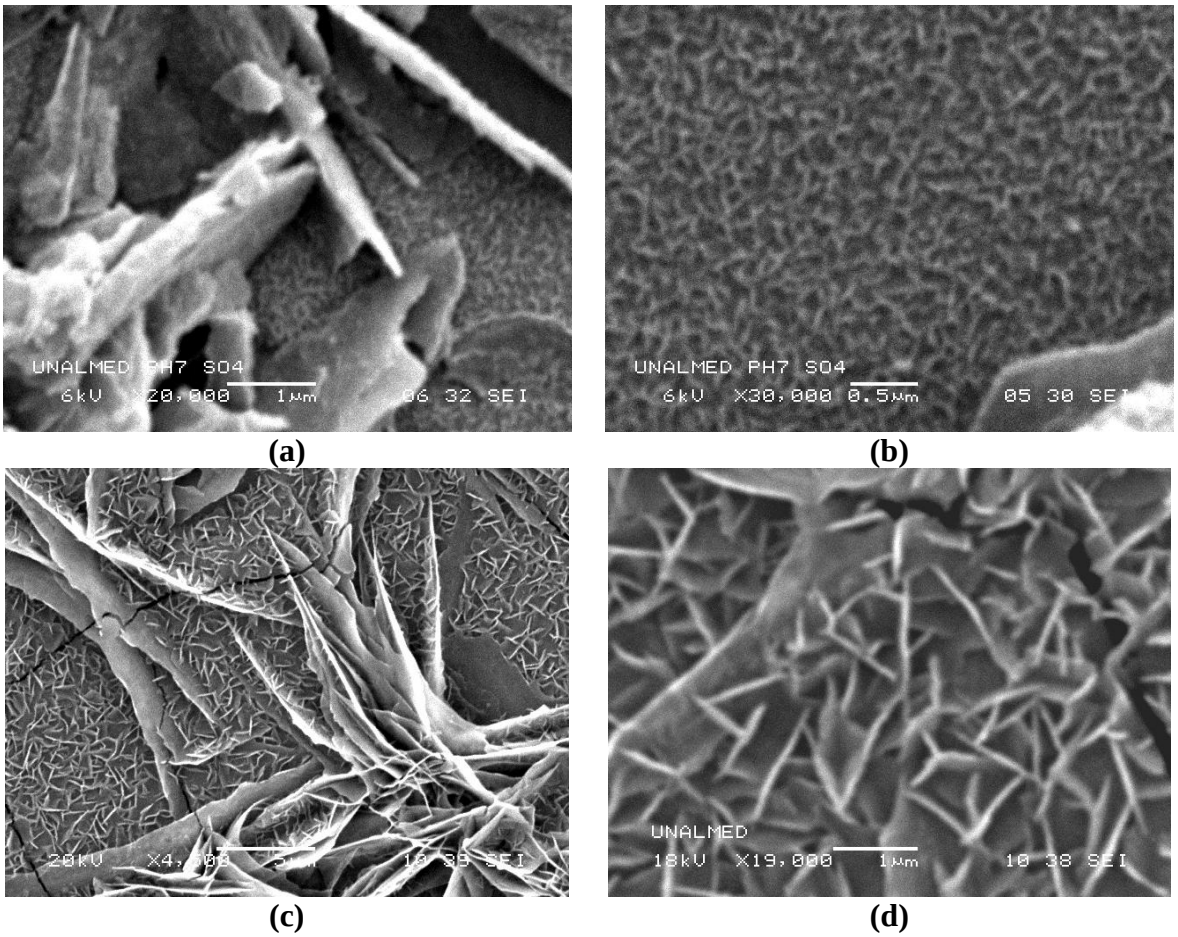

(a) **(b)** **(c)** **(d)**

Figure 5. SEM image of the electrodeposited films obtained in sulphate media (0.1M 1-methyl-imidazole + 0.2M Na_2SO_4), (a) and (b) pH = 7, (c) and (d) pH = 8.

SEM images clearly showed the influence of pH and anion on the morphology, distribution and growth of particles in the obtained deposits. Similar observations have already been made concerning the polarisation and transients of I *vs* t results. It appears that in the presence of SO_4^{2-}, GR and the oxy-hydroxide formed and grew slowly. This allowed time for maximum particle growth and better organization, resulting mainly in platelet forms. In contrast, in Cl^- media particle nucleation is quicker, stimulating the formation of smaller particles and agglomerates arranged in a globular array.

The changes in particle sizes and in the morphology of the deposits obtained at the different electrodeposition conditions can be explained by the differences found in the nucleation and growth rates of the deposit attained according to the type of electrolyte used. It can be expected lower particles size in the electrolyte which favors the nucleation rather than growth of the grains. This is the case of chloride electrolyte. It was observed in the polarization curves and transients of *I vs. t* results that lower polarization is required and more quickly stead-state is reached when iron oxide deposits are obtained in chloride electrolyte than in sulphate. This means that less energy is necessary to nucleation of new

phase. This phenomenon supports the idea that in the chloride electrolyte the nucleation of oxide particles is favored over growth. While in sulphate electrolyte more energy or superior supersaturation is required for nucleation of new phase; consequently the nuclei already formed tends to growth. It is important to emphasis that effect of anion in the size of particles is more evident than the changes in pH values.

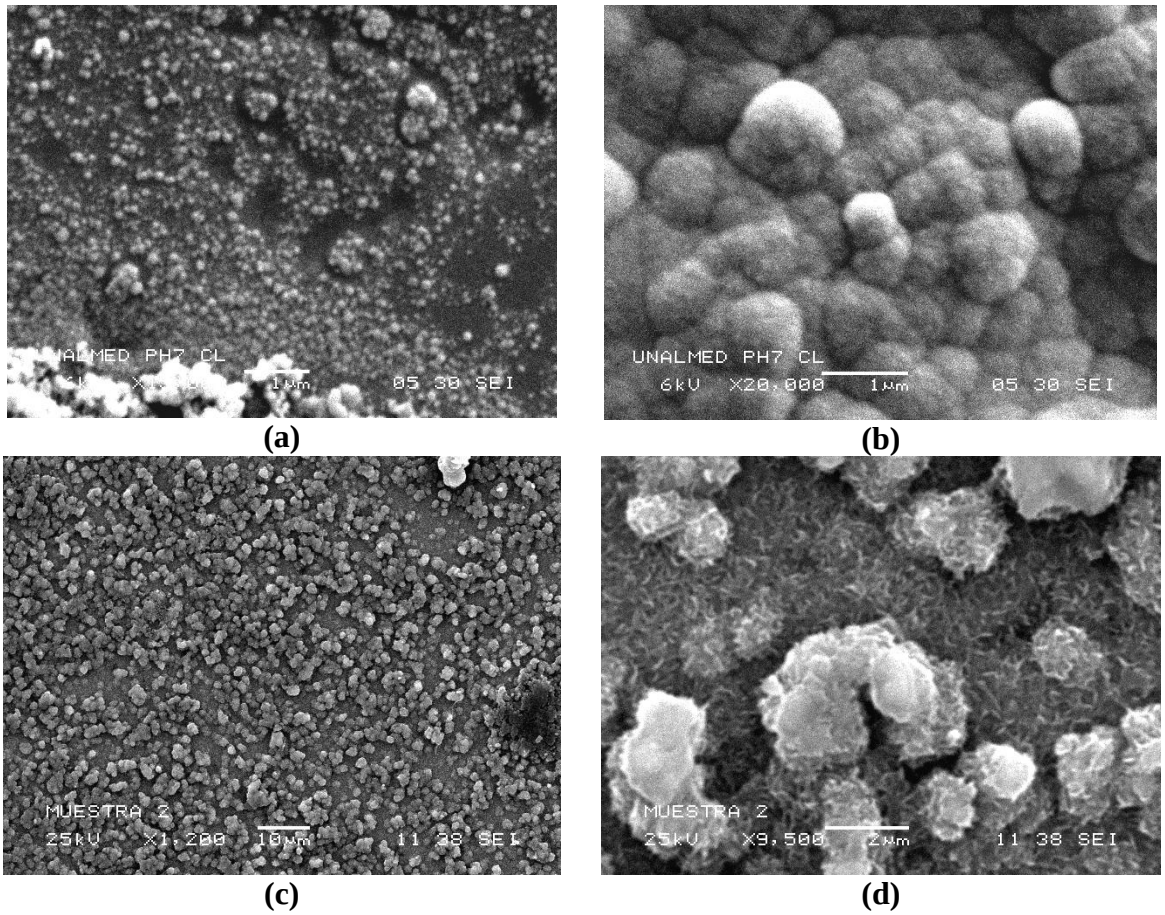

Figure 6. SEM image of the electrodeposited films obtained in chloride media (0.1M 1-methyl-imidazole + 0.4M NaCl), (a) and (b) pH = 7, (c) and (d) pH = 8.

3.3. Electrochemical impedance

Figure 7 shows the impedance diagrams done in potentiostatic mode at different anodic potentials. These potentials were selected from the polarisation curves during the electrodeposition process in Cl^- electrolyte at pH 8. Similar impedance diagrams were obtained in SO_4^{2-} media. The impedance at open circuit potential (OCP) is constituted by a line with an inclination angle superior to 45º. This behaviour is characteristic of diffusion processes in a semi-infinite layer. Under anodic polarisation conditions, the impedance diagrams show a small capacitive loop at high frequencies. These capacitive loops increase slightly in size when polarisation is increased and film deposition is induced. The capacitive loop at high frequencies corresponds to charge transfer resistance in parallel with double layer capacitance. At intermediary frequency values, lineal behaviour is observed, while at

the limit of very low frequencies a completely open capacitive loop is observed. Impedance behaviour at intermediate and low frequencies is characteristic of diffusion through the finite diffusion layer when diffusion is limited by absorbed compounds [26]. According to the impedance measurements, the diffusion processes significantly influence the electrodeposition kinetics of the oxy-hydroxide films; this influence is observed during both the precursor formation of green rust and the formation of the final layer of oxy-hydroxide.

According to the mechanism of green rust formation proposed by Génin *et al* [14-16] and by Peulon for the oxy-hydroxide electrodeposition [10-12] on inert substrates, the electrochemical co-deposition of goethite and lepidocrocite can be given by the following reactions:

$$6Fe(II) \rightarrow [Fe_4(II).Fe_2(III).(OH)_{12}].[A.2H_2O] \quad (1)$$

$$[Fe_4(II).Fe_2(III).(OH)_{12}].[A.2H_2O] \rightarrow 6\ (\alpha\text{-}\gamma)\text{-}FeOOH \quad (2)$$

The results obtained in this study show that the compound responsible for the shoulder observed in the polarisation curves is the green rust (GR) $[Fe_4(II).Fe_2(III).(OH)_{12}].[A.2H_2O]$, where A can be Cl^- or SO_4^{2-}, depending on the electrolyte used.

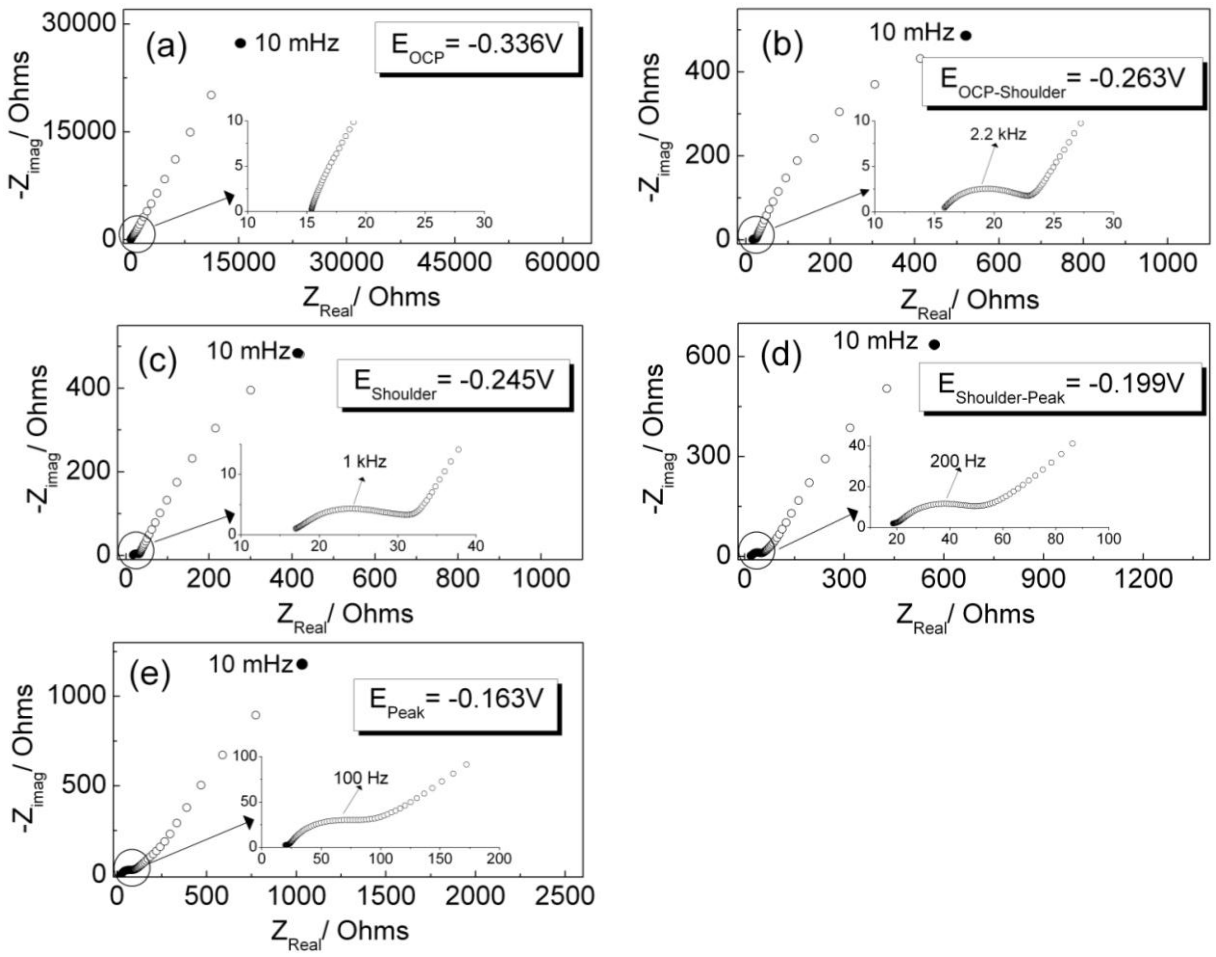

Figure 7. Impedance at different potentials selected from the anodic polarisation curve during electrodeposition of the iron oxyhydroxide films in chloride media (0.1M 1-methyl-imidazole + 0.4M NaCl), pH = 8.

Green rust is the precursor from which the further oxidation of Fe^{2+} ions and subsequent goethite and lepidocrocite formation occurred. The diffusion of the electroactive species toward the metal - electrolyte interface plays an important role in the formation of GR and oxy-hydroxide layers. In the case of GR formation, an excess of dissolved Fe^{2+}ions should exist in the metal - electrolyte interface [15, 16]. Considering that the electrode is anodic polarised, the excess of Fe^{2+}ions in solution is guaranteed by the migration of the dissolved Fe^{2+} ions towards the electrode surface. The Fe^{2+} ions may take the form of $HFeO_2^-$ since there is an excess of OH^- around the electrode during anodic polarisation and only negative charge are electrostatic attracted by the electrode. Once the excess of Fe^{2+} ions is guaranteed in the metal – electrolyte interface, the green rust formation occurs easily. In this way, the Cl^- or SO_4^{2-} ions have to migrate toward the electrode, induced by the anodic polarisation. Since Cl^- ions are smaller in size and have a higher oxidation potential that the SO_4^{2-} ions, the nucleation and growth of the oxy-hydroxide layer will be quicker in the presence of chlorides than in the presence of sulphates.

As anodic polarisation advances, the electrodeposited film increases in thickness, and diffusion of the electroactive species through the film is slow. Consequently, the excess of Fe^{2+} ions around the electrode is no longer guaranteed and the oxidation reaction results mainly in the transformation of green rust into goethite and lepidocrocite, reaction (2), at this point of polarisation anodic current reach a peak. Further oxidation processes is not kinetic favourable because the oxide layer is low conductive and diffusion through the layer become more difficult, then anodic current diminish after the peak.

4. CONCLUSIONS

The electrodeposition of iron oxy-hydroxides from chloride and sulphate solutions on inert substrates was successfully achieved. The deposits were stable and adherent and consisted of a mixture of good quality crystalline goethite, akaganeite and lepidocrocite. The experimental results presented in this work showed that the electrodeposition of iron oxy-hydroxides occurs, firstly through formation of a green rust film, characterised by a shoulder in the polarisation curves, and subsequently through formation of a porous iron oxy-hydroxide film. The type of anion and the pH of the electrolyte played an important role in the formation and further transformation of the iron oxides compounds on the film. It was corroborated that the Cl^- ions and high pH stimulated the green rust and final oxy-hydroxide film formation, been the goethite and akaganeite the main compounds present in the film, while the SO_4^{2-} ions and low pH retarded the formation of the film, constitutive mainly by lepidocrocite and akaganeite. The diffusion of the Fe^{2+}, Cl^- and SO_4^{2-} ions through the film controlled the kinetic of the electrodeposition process.

ACKNOWLEDGMENTS

The authors are grateful to the support given by the Colombian agency Colciencias, the “Centro de Excelencia en Nuevos Materiales (CENM)” and the "*Programa de Sostenibilidad 2013-2014”* of the Universidad de Antioquia.

References

1. S. Nasrazadani, *Corros. Sci*. 39 (1997) 1845.
2. R. M. Cornell, U. Schwertmann, The Iron Oxides: structures, properties, reactions, occurrences and uses, Wiley - VCH Verlag Gmbh & Co, KGaA, Weinheim, 2003.
3. C.A. Barrero, A.L. Morales, J. Mazo-Zuluaga, F. Jaramillo, D.M. Escobar, C. Arroyave, J. Tobón, P.M. Montoya, L. Osorio, R.E. Vandenberghe, J.M. Greneche, *Rev. Metal. Vol. Extraordinario* (2003) 62.
4. H.J. Masterson, J.G. Lunney and M.D. Coey, *J. Magn. Magn. Mater*. 115 (1992) 155.
5. M. Ouyang and H. Hiraoka, *Mater Res. Bull*. 32 (1997) 1099.
6. F. Yubero, M. Ocana, A. Justo, L. Contreras and A. Gonzalez-Elipe, *J. Vac. Sci. Technol. A Vac. Surf. Films* 18 (2000) 2244.
7. M. Rajendran, M.G. Krishna and A.K. Bhattacharya, *Int. J. Mod. Phys*. B 15 (2001) 1246.
8. G. M. da Costa, E. De Grave, P. M. A. de Bakker and R. E. Vandenberghe, *J. Solid State Chem*. 113 (1994) 405.
9. T. S. Chin and N. C. Chiang, *J. Appl. Phys*. 81 (1997) 5250.
10. S. Peulon, L. Legrand, H. Antony, A. Chaussé, *Electrochem. Comm*. 5 (2003) 208.
11. S. Peulon, H. Antony, L. Legrand, A. Chaussé. *Electrochim. Acta* 49 (2004) 2891.
12. H. Antony, S. Peulon, L. Legrand, A. Chaussé. *Electrochim. Acta* 50 (2004) 1015.
13. K. W. Chung, K. B. Kim, S. H. Han and H. Lee. *J. Electrochem. Soc*. 152 (2005) C560.
14. Ph. Refait and J.-M. R. Génin. *Corros. Sci*. 34 (1993) 797.
15. S. H. Drissi, Ph. Refait, M. Abdelmoula and J.-M. R. Génin. *Corros. Sci*. 37 (1995) 2025.
16. J.-M. R. Génin, A. A. Olowe, Ph. Refait and L. Simon. *Corros. Sci*. 38 (1996) 1751.
17. M. Yamashita, T. Shimizu, H. Konishi, J. Mizuki, H. Uchida. *Corros. Sci*. 45 (2003) 381.
18. D.C. Cook,R. Balasubramanian, S.J. Oh, M. Yamashita, *Hyperfine Interact*. 122 (1999) 59.
19. H. D. Ruan, R. L. Frost, J. T. Kloprogge, L. Doung. *Spectrochim. Acta* A 58 (2002) 967-981.
20. [20] N. A. Hakeem, A. B. Basily, N. Sagr, M. A. Moharram. *J. Mater. Sci.* 5 (1986) 4-6.
21. B. Weckler and H.D. Lutz, *Eur. J. Solid State Inorg. Chem*. 35, (1998), pp. 531-544.
22. D. L. A. de Faria, S. Venancio Silva and M. T. de Oliveira. *Journal of Raman Spectroscopy*, vol. 28, (1997) 873-878.
23. F. Dubois, C. Mendibide, T. Pagnier, F. Perrard, C. Duret. *Corrosion Science*, 50 (2008) 3401–3409.
24. S. Pineau, R. Sabot, L. Quillet, M. Jeannin, Ch. Caplat, I. Dupont-Morral, Ph. Refait, *Corrosion Science*, 50 (2008) 1099-1111.
25. C. Rémazeilles, P. Refait, *Corrosion Science* 49 (2007) 844–857.
26. J. Bisquert, G. Garcia-Belmonte, F. Fabregat-Santiago, P. Bueno. *J. Electroanal. Chem*. 475 (1999) 152.

© 2013 by ESG (www.electrochemsci.org)